

Analytical modeling of saturated zone head response to evapotranspiration and river-stage fluctuations

Bwalya Malama *, Brady Johnson

CGISS & Department of Geosciences, Boise State University, Boise, ID, USA

ARTICLE INFO

Article history:

Received 13 April 2009

Received in revised form 6 November 2009

Accepted 3 December 2009

This manuscript was handled by P. Baveye, Editor-in-Chief

Keywords:

Evapotranspiration

Unconfined aquifer

Phreatophyte

Hydraulic conductivity

SUMMARY

We investigate the response of the saturated zone (unconfined aquifer) to evapotranspiration (ET) flux at ground surface. We neglect fluid flow and storage in the unsaturated zone and treat ET as a sinusoidal forcing function at the watertable. The linearized kinematic condition is imposed at the watertable. Analytical solutions are developed for the case of flow in a domain of (a) semi-infinite extent to simulate response in a domain bounded by a river and (b) infinite lateral extent to simulate the response in a domain with no river boundaries. These solutions are fitted to observed groundwater head fluctuations recorded in observation wells at the Boise Hydrogeophysical Research Site in Idaho and the Larned Research Site in Kansas. Estimates of the amplitude of the ET flux, aquifer hydraulic conductivity, specific storage and specific yield are obtained and these compare well to published results from pumping tests conducted at the site. The field exercise is used to explore the potential for using groundwater head fluctuations to estimate ET and hydraulic parameters of unconfined aquifers.

© 2009 Elsevier B.V. All rights reserved.

Introduction

The principal mechanism of groundwater discharge in arid and semi-arid regions is through evapotranspiration (ET) from bare soil and phreatophytes (Nichols, 1993). Phreatophytes are deep-rooted plants, such as cottonwood (*Populus* spp.), greasewood (*Sarcobatus vermiculatus*), saltcedar (*Tamarix chinensis*), and Arizona mesquite (*Prosopis velutina*), that obtain water from a permanent ground supply or from the saturated zone. Hence, in riparian zones with predominantly phreatophyte vegetation, it is common for hydrographs from wells installed in the saturated zone to display a characteristic pattern of diurnal fluctuations (Butler et al., 2007a). White (1932) developed a method for estimating the ET flux associated with groundwater consumption by phreatophytes from these diurnal fluctuations of saturated zone water levels. In this approach, ET is computed according to the relation $ET = S_y \delta s / T + Q$ where S_y is specific yield, δs [L] is the residual drawdown between the two adjacent maxima of groundwater level fluctuations, T is the time elapsed between the two maxima and Q [L/T] is the net recovery rate of groundwater. Loheide et al. (2005) used a saturated–unsaturated flow numerical simulation to assess the usefulness of the method of White (1932) and concluded that the method tends to significantly overestimate ET if the effects of depth to

watertable and drainage time on specific yield are neglected. They provided guidelines for estimating specific yield for use with the method of White (1932) to more accurately quantify ET.

Recently, Gribovszki et al. (2008) modified the method of White (1932) in an attempt to more correctly estimate the net recovery rate of groundwater, Q . Using the Dupuit approximation for saturated zone flow they were able to relate Q to water level fluctuations. For saturated zone flow that is predominantly vertical, they proposed the relation $Q = K_z(H - h)/\ell$, where h is the groundwater elevation, H the hydraulic head at some depth ℓ below a reference level and K_z is the vertical hydraulic conductivity of the saturated zone. The parameter ℓ can be taken to equal the thickness of the aquifer, and H can be estimated from predawn data where ET is negligible, as $H = h - \ell S_y \delta s / (TK_z)$.

None of the works cited above have developed an analytical model to describe the diurnal head fluctuations of groundwater due to evapotranspiration and step changes in river stage. It is therefore, the objective of this work to develop analytical models describing these diurnal head fluctuations of groundwater by solving the transient saturated zone flow problem in which the ET flux is treated as a forcing function at the watertable and river stage is imposed as a time varying Dirichlet boundary condition. We solve the saturated zone flow problem on lateral domains of (a) semi-infinite and (b) infinite extent. The solution obtained on the semi-infinite interval simulates the response in a domain bounded by a river, whereas that on the infinite interval simulates the response in a domain with no river boundaries. In the development of these solutions, it is assumed that all the water discharged

* Corresponding author. Present address: Montana Tech of University of Montana, Department of Geological Engineering, Butte, MT, USA. Tel.: +1 406 496 4272; fax: +1 406 496 4260.

E-mail address: bmalama@mtech.edu (B. Malama).

Nomenclature

K_z	vertical hydraulic conductivity of aquifer (LT^{-1})	t	elapsed time since R_n became positive (T)
K_x	horizontal hydraulic conductivity of aquifer (LT^{-1})	z	vertical distance from aquifer base (L)
S_s	specific storage of aquifer (L^{-1})	Q	evapotranspiration amplitude (LT^{-1})
S_y	specific yield	p	Laplace transform parameter
b	initial saturated thickness of aquifer (L)		
s	head change (L)		

through evapotranspiration comes entirely from the saturated zone. This assumption was adopted by White (1932) and is valid in riparian zones where phreatophytes are the predominant means of groundwater discharge to the atmosphere. In fact, Shah et al. (2007) found, through numerical simulations coupling vadose and saturated zone flow, that if the watertable lies within a half meter below land surface, almost all ET comes from groundwater.

In developing the solutions presented herein, the watertable is treated in the manner of Neuman (1972) as a moving material boundary and flow in the unsaturated zone is ignored, given that the drawdowns induced by evapotranspiration are typically small. The model results were generated with a piecewise sinusoidal ET forcing function at the watertable. The piecewise sinusoidal nature of the evapotranspiration flux is supported by ground station measurements of latent heat flux (Bisht et al., 2005; Batra et al., 2006) as well as by direct measurements of plant sap flow (Cienciala et al., 2000; O'Brien et al., 2004), and has been used by Puma et al. (2005). A significant contribution of this work is that when evapotranspiration is well characterized, the solutions can be used to characterize the saturated zone by an inversion scheme of the diurnal head fluctuations. The converse is also true, that if the unconfined aquifer is well characterized, the solution may be used to estimate surface evapotranspiration. Additionally, it is demonstrated herein, that hydraulic parameters and the parameters that characterize the ET flux can be determined jointly, given sufficient data. However, the problem is less ill-posed if one set of parameters is well characterized by some other method. In the sections that follow we present the mathematical formulation of the problem, develop and discuss the solutions and fit the model to field data from Loheide et al. (2005) and Butler et al. (2007a).

Mathematical formulation and solution

We consider here the response of the hydraulic head in an unconfined aquifer (saturated zone below watertable) to an areal fluid flux at the watertable. We will consider two-dimensional flow in an aquifer of finite vertical ($0 < z < b$) extent and (a) semi-infinite lateral extent ($0 < x < \infty$) bounded by a river at $x = 0$, as depicted in Fig. 1a and (b) infinite lateral extent ($-\infty < x < \infty$), as depicted in Fig. 1b. For the flow problems considered here, the head change, s , from an initial static state is governed by the equation

$$\frac{\partial s_D}{\partial t_D} = \kappa \frac{\partial^2 s_D}{\partial x_D^2} + \frac{\partial^2 s_D}{\partial z_D^2}, \quad (1)$$

expressed in nondimensional form, where $s_D = s/H_c$, H_c is some characteristic head to be defined later, $\kappa = K_x/K_z$, $t_D = \alpha_z t/b^2$, $\alpha_z = K_z/S_s$, $x_D = x/b$, $z_D = z/b$, (x, z, t) are the space-time coordinates, b is the initial thickness of the saturated zone, K_x and K_z are horizontal and vertical hydraulic conductivities, respectively, and S_s is the specific storage. For all the cases discussed below, Eq. (1) is solved subject to the initial condition

$$s_D(x_D, z_D, t_D = 0) = 0, \quad (2)$$

and the boundary conditions

$$\frac{\partial s_D}{\partial z_D} \Big|_{z_D=0} = 0, \quad (3)$$

at the base of the aquifer, implying no leakage from the underlying formation, and

$$-\frac{\partial s_D}{\partial z_D} \Big|_{z_D=1} = \frac{1}{\sigma} \frac{\partial s_D}{\partial t_D} \Big|_{z_D=1} - f_D(t_D), \quad (4)$$

at the watertable, where $\sigma = bS_s/S_y$, S_y is specific yield, $z_D = 0$ is the base of the aquifer, $z_D = 1$ is the initial position of the watertable and $f_D(t_D)$ is the ET flux function at the watertable expressed in non-dimensional form. For $f_D(t_D) = 0$ Eq. (4) is simply the linearized kinematic condition used by Neuman (1972) in the delayed gravity response model for unconfined aquifer flow. The watertable is treated as a moving material boundary and flow in the unsaturated zone is ignored. In the following two sections we outline the additional boundary conditions needed to solve the above flow problem as well as the respective solutions for the semi-infinite and infinite flow domains.

ET–river–groundwater interaction

The solution developed here is for two-dimensional flow in an unconfined aquifer, bounded by a river, in response to evapotranspiration and temporal fluctuations in river stage. For this case, Eq.

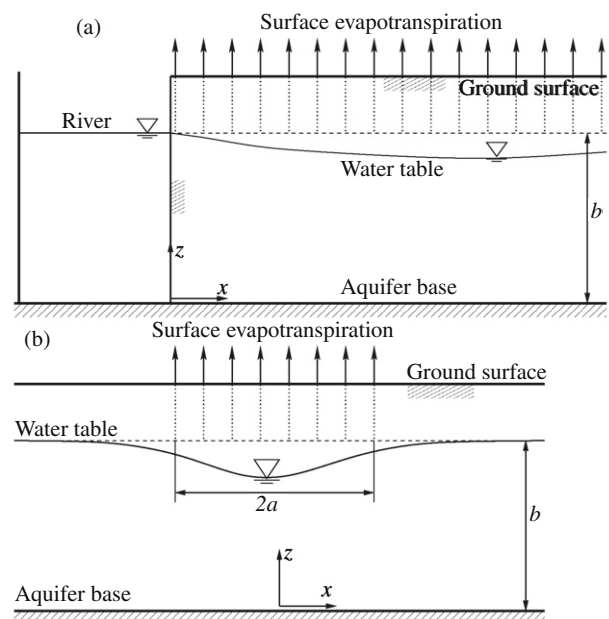


Fig. 1. Schematic of the conceptual model of the evapotranspiration and subsurface flow problem for the case of (a) a semi-infinite flow domain bounded by a river, and (b) a domain of infinite lateral extent, with evapotranspiration from a finite strip of surface vegetation.

(1) is solved on the semi-infinite domain $0 < x_D < \infty$ subject to the additional Dirichlet boundary conditions

$$s_D(0, z_D, t_D) = r_D(t_D), \tag{5}$$

at the edge of the river, and

$$\lim_{x_D \rightarrow \infty} s_D(x_D, z_D, t_D) = 0. \tag{6}$$

The function $r_D(t_D)$ describes the temporal variations in river stage. The boundary condition given in Eq. (6) implies that there are no head fluctuations far from the river.

Using Laplace (in t_D) and Fourier sine (in x_D) transforms, it can be shown (see Appendix “Solution of flow equation”) that the solution to this flow problem is

$$\bar{s}_D^* = \bar{s}_{D,r}^* + \bar{s}_{D,et}^*, \tag{7}$$

where $\bar{s}_{D,r}^*$ is the aquifer response to river stage fluctuations, and is given by

$$\bar{s}_{D,r}^* = \frac{2}{\pi} \frac{\kappa \zeta}{\eta^2} \left[1 - \frac{p}{\sigma} \bar{u}_D^* \right] \bar{r}_D(p), \tag{8}$$

and $\bar{s}_{D,et}^*$ is the aquifer response to the ET forcing, and is given by

$$\bar{s}_{D,et}^* = \frac{2}{\pi \zeta} \bar{u}_D^* \bar{f}_D(p). \tag{9}$$

The function $\bar{u}_D^*(\zeta, z_D, p)$ is given by

$$\bar{u}_D^*(\zeta, z_D, p) = g(\zeta, p) \cosh(\eta z_D), \tag{10}$$

where p and ζ are the Laplace and Fourier sine transform parameters, respectively, $\eta^2 = p + \kappa \zeta^2$, $\bar{s}_D^* = \mathcal{L}\mathcal{L}\{s_D\}$ the double Laplace and Fourier sine transform of dimensionless head fluctuation, $\bar{r}_D(p) = \mathcal{L}\{r_D(t_D)\}$ and $\bar{f}_D(p) = \mathcal{L}\{f_D(t_D)\}$ are the Laplace transforms of dimensionless river stage and evapotranspiration flux functions, respectively, and

$$g(\zeta, p) = [\eta \sinh(\eta) + (p/\sigma) \cosh(\eta)]^{-1}. \tag{11}$$

This solution describes temporal head changes in the saturated zone in response to the forcing functions $f(t)$ at the watertable, and $r(t)$ at $x = 0$. The inverse transforms are obtained numerically.

ET-groundwater interaction

The solution developed here is for the diurnal head fluctuations of the unconfined aquifer in response to evapotranspiration only. The solution is useful far enough from the influence of, or in the absence of a river boundary. Eq. (1) is solved on the infinite domain $-\infty < x_D < \infty$, with the evapotranspiration flux function nonzero over the symmetric interval $x_D \in [-a_D, a_D]$ and vanishing identically elsewhere, with $a_D = a/b$ being the normalized half-width of the vegetation strip. Using the Laplace and Fourier transforms, it can be shown that the solution to this problem is given by

$$\bar{s}_{D,et}^*(\zeta, z_D, t_D) = \frac{\sin(a_D \zeta)}{\pi \zeta} \bar{u}_D^* \bar{f}_D(p), \tag{12}$$

where $\bar{s}_D^* = \mathcal{L}\mathcal{L}\{s_D\}$ is the double Laplace and Fourier transform of dimensionless head fluctuation, \bar{u}_D^* has the same form as that in Eq. (10) and ζ is the Fourier transform parameter. The inverse transforms for this case are also obtained numerically.

The ET flux function

We assume here that all the water discharged through evapotranspiration comes entirely from the saturated zone. We also neglect the contribution of the vadose zone to the storage of water and to evapotranspiration. This assumption was adopted by White (1932) who found it to be valid for riparian zones where phreato-

phytes are the predominant means of groundwater discharge to the atmosphere. Recently, Shah et al. (2007) found, through numerical simulations coupling vadose and saturated zone flow, that if the watertable is within a half meter below land surface, almost all ET comes from groundwater. Hence, for our purposes, it is sufficient to assume that the ET flux function $f(t)$ is obtainable from the Priestley–Taylor equation which has the form (Batra et al., 2006)

$$\lambda ET = \phi \left(\frac{\Delta}{\Delta + \gamma} \right) (R_n - G), \tag{13}$$

where λ is the latent heat of vaporization of water (Jkg^{-1}), ET is evapotranspiration mass flux ($\text{kg m}^{-2} \text{s}^{-1}$), ϕ is the parameter that accounts for aerodynamic and canopy resistance, Δ the slope of the saturated vapor pressure curve (a function of air temperature, T_a), γ the psychrometric constant (kPa/K), R_n the net heat radiation (Wm^{-2}), and G is the soil heat flux (Wm^{-2}). Bisht et al. (2005) proposed a sinusoidal model for estimating the diurnal net radiation cycle following the work of Lagouarde and Brunet (1993) on the diurnal cycle of surface temperature. The model of Bisht et al. (2005) has the form

$$R_n(t) = R_{n,max} \sin(\omega t), \tag{14}$$

where t is the elapsed time since t_{rise} , $R_{n,max}$ is the maximum value of R_n estimated during the day, $\omega = \pi/t_{day}$, $t_{day} = t_{set} - t_{rise}$ and, t_{rise} and t_{set} are the respective local times at which R_n becomes positive and negative. Additionally, using the scheme of Moran et al. (1989) and Batra et al. (2006) show that soil heat flux, G , is directly proportional to net radiation. It follows then that, of a single diurnal cycle, the evapotranspiration function, $f(t)$, has the following piecewise smooth form Batra et al., 2006

$$f(t) = \frac{ET}{\rho} = \begin{cases} Q \sin(\omega t) & \forall t \in [0, t_{day}] \\ 0 & \forall t > t_{day}, \end{cases} \tag{15}$$

where ρ is the density of water and Q is the amplitude of the evapotranspiration flux at the watertable, given by Batra et al., 2006

$$Q = \frac{R_{n,max} \phi \Delta}{\rho \lambda (\Delta + \gamma)} (1 - 0.583 e^{-2.13 NDVI}), \tag{16}$$

where NDVI is the normalized vegetation index. Fig. 2 shows the function $f(t)$ over a 24 h period. The piecewise nature of the evapotranspiration flux is supported by ground station measurements of latent heat flux (Bisht et al., 2005; Batra et al., 2006) as well as by direct measurements of plant sap flow (Cienciala et al., 2000; O’Brien et al., 2004) and has been used by Puma et al. (2005). In nondimensional form, with the characteristic head defined as $H_c = Qb/K_z$, the evapotranspiration flux function is

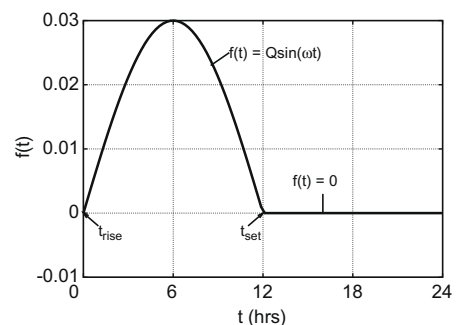


Fig. 2. The piecewise smooth function of the evapotranspiration flux at the watertable.

$$f_D(t_D) = \begin{cases} \sin(\omega_D t_D) & \forall t_D \in [0, t_{D,\text{day}}] \\ 0 & \forall t_D > t_{D,\text{day}}, \end{cases} \quad (17)$$

where $\omega_D = \omega b^2 / \alpha_z$ and $t_{D,\text{day}} = \alpha_z t_{\text{day}} / b^2$.

Model predicted aquifer response

It is usually the case that the diurnal head fluctuations are measured with a pressure transducer placed in an observation well that is screened over the entire saturated thickness. In this case, the measured head fluctuations are depth averaged. One then has to replace \bar{u}^* with

$$\langle \bar{u}_D^*(\xi, p) \rangle = \frac{g(\xi, p)}{\eta} \sinh(\eta), \quad (18)$$

in Eqs. (8), (9) and (12). Additionally, with the ET flux function defined according to Eq. (17), the drawdown response, $s_{D,\text{cy}}(z_D, t_D)$, for a complete diurnal cycle is

$$s_{D,\text{cy}}(z_D, t_D) = \begin{cases} s_D(z_D, t_D) & \forall t_D \in [0, t_{D,\text{day}}] \\ s_D(z_D, t_D) + s_D(z_D, t_D - t_{D,\text{day}}) & \forall t_D > t_{D,\text{day}}, \end{cases} \quad (19)$$

where the recovery phase requires addition of the term $s_D(z_D, t_D - t_{D,\text{day}})$ since the sine function is negative. All the results presented below are computed using Eq. (19).

The inverse Laplace and Fourier transforms of aquifer head response are obtained numerically in this work. The Laplace transforms are inverted using the fixed Talbot (FT) algorithm (Abate and Valko, 2004) whereas inverse Fourier transforms are obtained by numerical integration routines available in MATLAB. All the computations are performed in MATLAB and the routines developed for this purpose are available from the authors upon request. For all the model results presented in this section, we set $K_x = K_z = 4 \times 10^{-4}$ m/s, $S_s = 3 \times 10^{-5}$ m⁻¹, $S_y = 0.25$, and $b = 20$ m. For the infinite domain (ET only) flow problem, the vegetation strip was restricted to a half-width of $a_D = 3.0$.

The plots in Fig. 3 show the variation of the predicted response of the aquifer at different vertical positions from the base of the saturated zone. The plots show the predicted response of the saturated zone for a domain of (a) semi-finite lateral, with a constant river head ($r_D(t_D) = 0$) and (b) infinite lateral extent. The depth average solution is also shown in each of the plots. In the figure, $z_D = 0.0$ and $z_D = 1.0$ correspond to the base of the aquifer and the initial position of the watertable, respectively. The response function plotted in the figure is periodic with a period of 1 day. Both plots indicate the obvious net upward flow of water initially, followed by a recovery period afterward. This is indicated by the

fact that drawdown at the watertable ($z_D = 1.0$) peaks first, with the time of peak drawdown shifting to the right with increasing depth from the watertable. The results in Fig. 3a, for the semi-infinite domain problem, were computed at $x_D = 5.0$, where as those in (b), for the infinite domain, were obtained at $x_D = 0$. Hence, the differences in magnitudes in the responses are due to the fact that results in (a) were obtained far from the river boundary (five times the saturated thickness), where as those in (b) were obtained directly in the center of the ET strip.

The depth averaged response, which corresponds to the response measured with a pressure transducer placed in a well that is screened across the entire saturated thickness, shows that after a full period (1 day), the recovery of the aquifer head is incomplete. The head residual at the end of a 24 h cycle, δs [L], can be used to estimate the groundwater consumption (net loss to atmosphere) by phreatophytes. The net volumetric groundwater consumption per unit area due to incomplete recovery during the period of zero ET, is given by $S_y \delta s$. The figure also shows that peak drawdown lags behind the peak evapotranspiration flux imposed at the watertable.

Fig. 4 shows the response of the saturated zone to ET at different lateral positions from (a) the edge of the river in the domain of semi-finite lateral extent and (b) from the center of the vegetated area in the domain of infinite extent. The depth averaged drawdown, $\langle s_D \rangle$, is plotted against time. The results in Fig. 4a show the expected increase in drawdown as one moves away from the river, which is a constant head Dirichlet boundary with $r_D(t_D) = 0$. Fig. 4b shows that maximum drawdown is at the center of the vegetated area. Some of the drawdowns for the river bounded domain are larger than those for the unbounded domain owing to the relative positions on the observation points: observation points far from the river boundary can show larger drawdowns than observation points in the unbounded domain that lie outside the vegetation strip responsible for aquifer head changes. It should be noted that the vegetation strip in the semi-infinite flow domain covers the entire half-space, where as that in the infinite flow domain problem, covers a finite strip as depicted in the conceptual models in Fig. 1.

Specific yield, S_y , is an important parameter in the control of the rate of watertable movement due to water flow into or out of the saturated zone. Fig. 5 shows the effect of the specific yield on response of the saturated zone to ET for the domain of (a) semi-finite and (b) infinite lateral extent. Both graphs show the expected result that media characterized by small values of S_y experience greater drawdown than those with larger values. This greater drawdown associated with small values of S_y in turn leads to larger drawdown residuals at the end of the diurnal cycle. It should be noted however, that the rate of recovery increases with decreasing

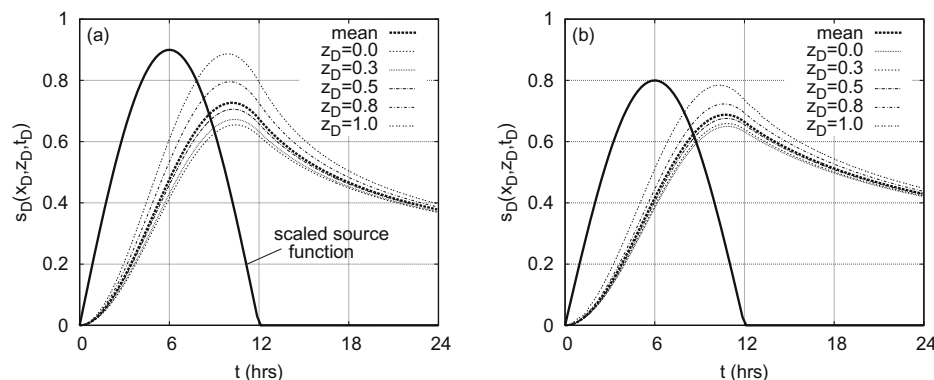


Fig. 3. Predicted diurnal fluctuation of dimensionless head in an unconfined aquifer. Response in domain of (a) semi-finite extent bounded by a river and (b) infinite lateral extent.

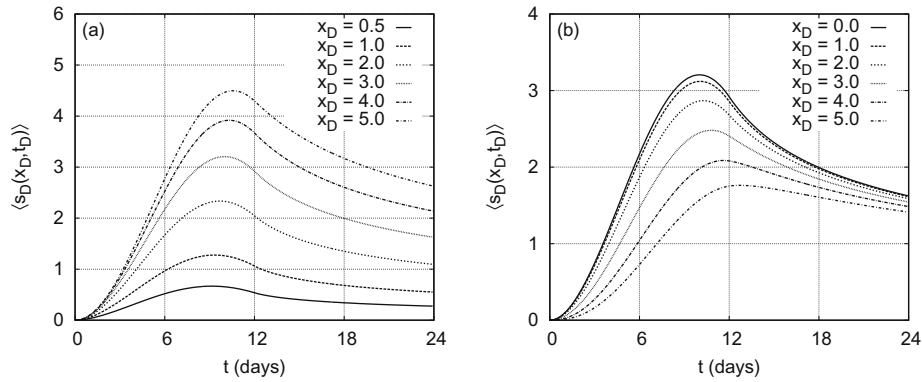


Fig. 4. Variation of aquifer response with x_D in domain of (a) semi-finite extent bounded by a river and (b) infinite lateral extent.

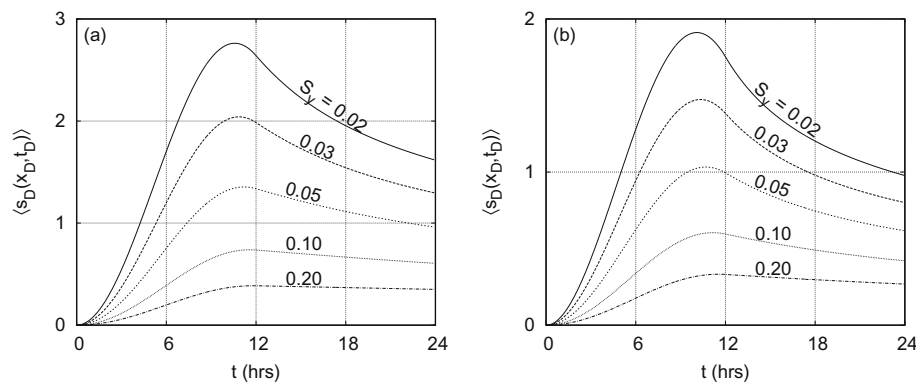


Fig. 5. The effect of specific yield, S_y , on head response to ET. Response in domain of (a) semi-finite extent bounded by a river and (b) infinite lateral extent.

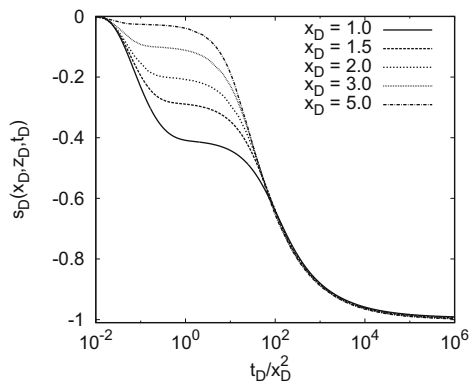


Fig. 6. Semi-log plot of unconfined aquifer response to step change in river stage for different distances from the edge of the river.

values of S_y , as indicated by the steeper slope of the recovery branch of the diurnal head response curve for smaller values of S_y in Fig. 5.

The response of the saturated zone to a unit step change in river stage, for the case where ET is negligible, is shown in Fig. 6 for different lateral positions from the edge of the river. The results shown in the figure are for the case where the head in the river is increased instantaneously at $t_D = 0$. The values plotted are negative because the convention used in this work is that head decreases, termed drawdown, due to flow out of the saturated zone, are positive. The results in the figure show that the model developed here predicts the delayed gravity response (Neuman,

1972), typically observed during pumping tests in unconfined aquifers, to step changes in river stage.

The results presented above all indicate that at the end of a diurnal cycle, the head in the saturated zone does not recover completely to its initial state even in the presence of a river boundary. The residual drawdown, δs , is associated with the net amount of water consumed by phreatophytes. This residual leads to a linear decrease in the saturated zone head as shown in Fig. 7. The model predicted response shown in the figure is at $x_D = 5.0$ m over (a) a 5-day period with $r(t) = 0$ for all t , and (b) a 10-day period with a 3 cm step change in river stage at 4.5 days. For the results shown, we have assumed the head residuals and the amplitude of the surface ET flux are constant over the 5 day period. The linear decrease in the saturated zone head predicted here has been observed in the data collected at the Larned Research Site (LRS) near Larned, Kansas, by Loheide et al. (2005) and Butler et al. (2007a). The slope of the trend is controlled by the head residual at the end of each daily cycle. Large residuals yield a steeper slope whilst small residuals yield a lower slope. Hence, the slope of the linear trend would decrease with decreasing x_D , the normalized distance from the edge of the river (constant head) boundary, since the results in Fig. 4a indicate that the head residual decreases with decreasing x_D . The slope of the linear trend would also decrease with increasing values of the specific yield, S_y , as smaller head residuals are associated with larger specific yield values as the model results in Fig. 5 indicate.

Application to field data

In this section we fit the model developed herein to data of diurnal head fluctuations obtained at (a) the Boise Hydrogeophysical

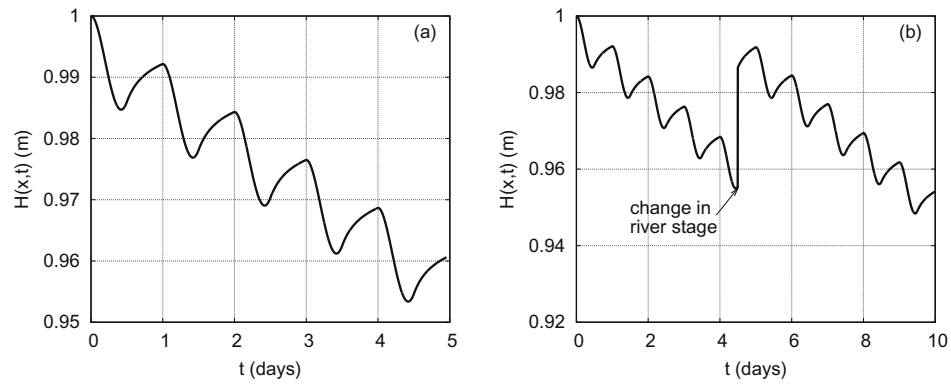


Fig. 7. Plot of diurnal fluctuations of hydraulic head at $x = 100$ m over (a) a 5-day period with $r(t) = 0$ for all t , and (b) a 10-day period with a 3 cm step change in river stage at 4.5 days.

Research Site (BHRS) in Boise, Idaho and (b) the Larned Research Site (LRS) in Larned, Kansas.

Boise hydrogeophysical research site

This site is situated next to the Boise river, which flows continuously throughout the year. The aquifer at the BHRS is unconfined

and is bounded to the southwest by the Boise River, and below by a clay unit, which is continuous at the site. The aquifer, with a vertical extent of about 16 m, consists of unconsolidated cobble and sand fluvial deposits (Barrash and Clemo, 2002; Barrash and Reboulet, 2004; Barrash et al., 2006). The river stage varies significantly from a winter low to a high following the spring snow melt in the mountains upstream of the research site. The vegetation at the site

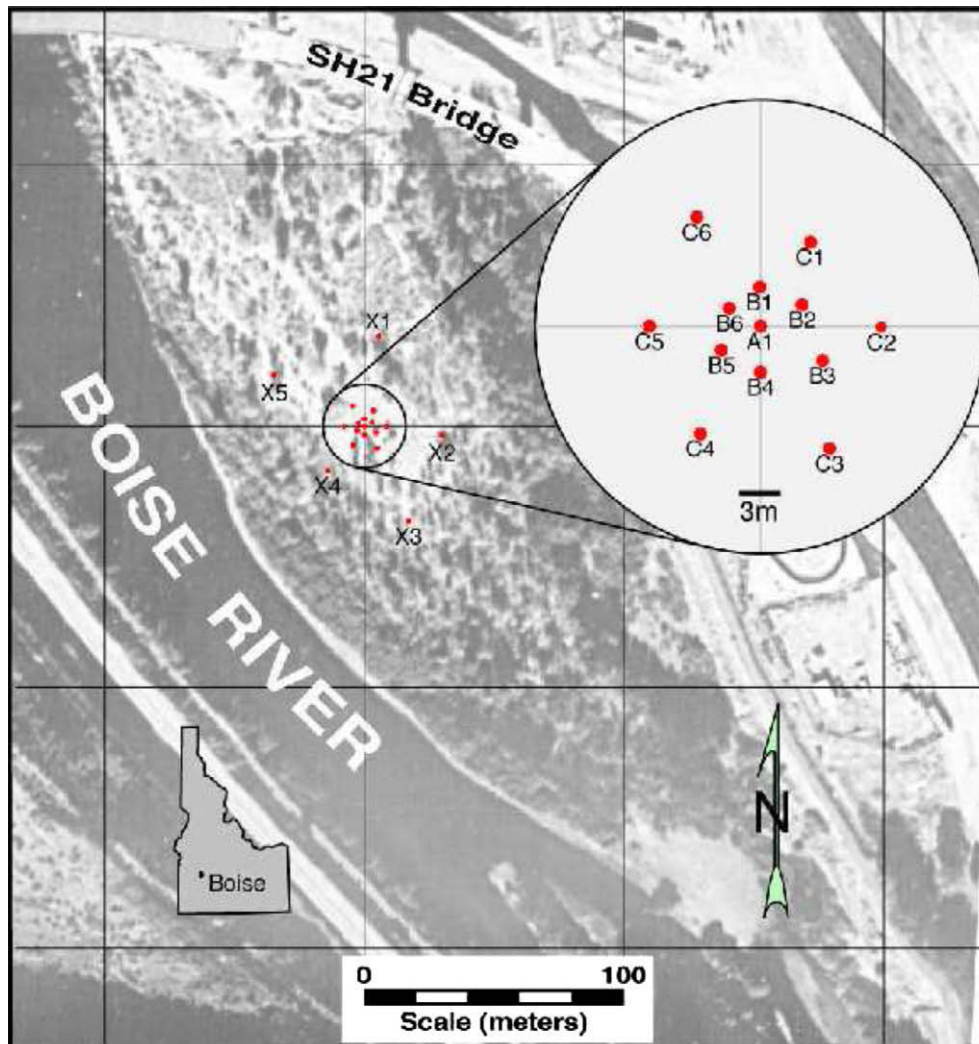


Fig. 8. Site layout of the BHRS showing the well-field and the Boise river (after Barrash and Reboulet, 2004). The diversion dam is to the southeast of site on the river.

is mostly Cottonwoods (*Populus* spp.), which are known phreatophytes. Fig. 8 shows the location of the site, as well as the wells in which the data analyzed here were collected.

We consider here the aquifer response data obtained over a 5-day period in the summer of 2008 at the BHRS. The data are shown in Fig. 9a. The data were obtained in a well located in the center of the well-field, at 75 m from the edge of the river. They show the response of the aquifer to river-stage fluctuations and evapotranspiration. The effect of river-stage change is most pronounced during the 1st day of data acquisition. Fig. 9b shows the fit of the solution developed herein on the semi-infinite domain, to the data. The parameters obtained from inversion of the data where the river-stage changes during the 1st, 3rd, and 4th days of data acquisition, hydraulic conductivity, and the amplitude of the evapotranspiration signal on each of the 5 days. These parameters were obtained as follows:

1. river-stage change, hydraulic conductivity, and evapotranspiration amplitude for days 1 and 2, were first obtained from the data collected on days 1 and 2,
2. the evapotranspiration amplitude and river-stage change during day 3 were estimated from day 3 data,
3. the evapotranspiration amplitude and river-stage change during day 4 were estimated from day 4 data, and
4. the evapotranspiration amplitude during day 5 were estimated from day 5 data.

The hydraulic conductivity determined from day 1 and 2 data was used for days 3, 4, and 5.

During the parameter estimation exercise, the specific storage and specific yield were fixed at $3.8 \times 10^{-6} \text{ m}^{-1}$ and 0.05, respectively, values determined from pumping test data. The hydraulic conductivity estimated from the data in Fig. 9 was $K = 3.4 \times 10^{-4} \text{ m/s}$, which is comparable to estimates from pumping test data for the site (Barrash et al., 2006). The aquifer was assumed to be isotropic. A summary of the estimated river-stage changes and the amplitudes of evapotranspiration, is given in Table 1. A piecewise constant function definition was used for the river-stage function, which corresponds to step-increases (or decreases) in river stage.

The model for the semi-infinite domain bounded by a river, fits the data well. This field exercise demonstrates that data collected from passive monitoring of wells can be used to estimate aquifer parameters, in particular, hydraulic conductivity. The model could also be used to invert data for daily ET amplitudes, as well as river-stage changes, where other methods of direct measurement are not available.

Larned Research Site

This site was established to study riparian zones characteristic of the High Plain region of the United States (Butler et al., 2007a). The site, as described in Butler et al. (2007a), is located adjacent to a USGS stream-gauging station on the Arkansas River near Larned, Kansas. It is known to overlie an unconfined, coarse-sand and gravel aquifer. The predominant phreatophyte vegetation at the site are cottonwoods (*Populus* spp.), with some mulberry (*Morus* spp.) and willow (*Salix* spp.), a combination representative of native riparian zone vegetation of the High Plain region (Butler et al., 2007a; West and Ruark, 2004).

The unconfined aquifer at the site is in direct hydraulic connection with the Arkansas River, which flows intermittently (Butler et al., 2007a). The model developed in “ET–river–groundwater interaction” would be used to model aquifer response during the periods of river flow, whereas that developed

Table 1
Estimated values of river-stage changes and daily amplitudes of evapotranspiration.

Day	r (m)	Q (mm/day)
1	0.129	3.8
2	0.129	3.5
3	0.133	3.3
4	0.137	3.1
5	0.137	2.5

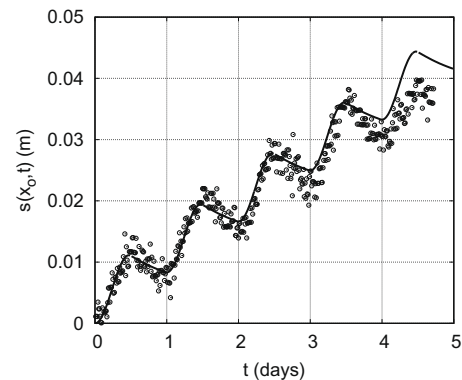


Fig. 10. Fit of the model to data collected at the Larned Research Site (data after Butler et al., 2007a).

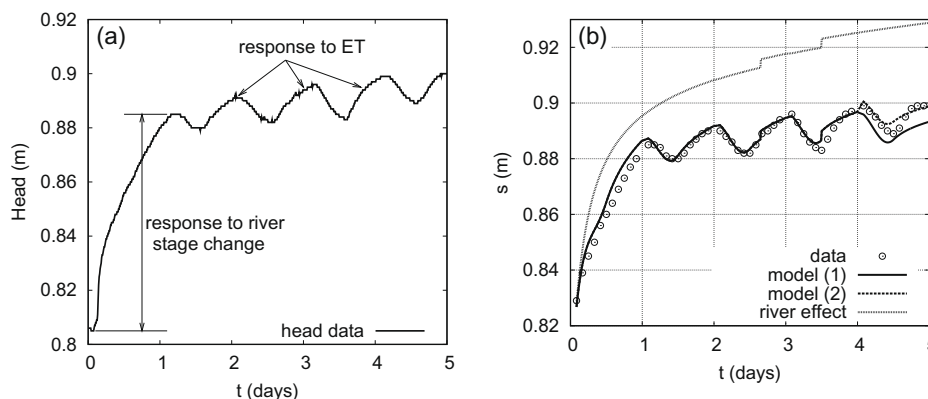


Fig. 9. (a) Head data collected at the Boise Hydrogeophysical Research Site and (b) model fit to the data reflecting the effects of both river-stage fluctuations and evapotranspiration (solid curve is for same ET amplitude for days 4 and 5, dashed is for different ET amplitudes for days 4 and 5, and dotted curve shows river stage effects).

in “ET–river interaction” would be used during periods of no river flow. Fig. 10 shows the fit of the model to measured diurnal head fluctuations in a watertable aquifer at the LRS for the 4-day period of July 14–18 in 2003. A constant daily ET amplitude was assumed for the whole 4-day period, which may explain the model deviation from data after day 2. In practice, the ET amplitude varies from day to day controlled chiefly by the daily maximum temperature. We used a constant value to simplify the analysis, though the model can handle the daily variability of ET amplitude.

The hydraulic parameters estimated by nonlinear least squares were $K_x = K_z = 6.31 \times 10^{-4}$ m/s, $S_s = 5.66 \times 10^{-5} \text{ m}^{-1}$, and $S_y = 0.196$. The amplitude of the ET signal, responsible for the observed groundwater head fluctuations, was estimated at $Q = 9.14 \times 10^{-8}$ m/s (7.9 mm/day). Since, as reported by Butler et al. (2007a), there was no flow in the Arkansas river during the 4-day period when the data were collected, we used the infinite lateral domain solution, with a riparian zone of finite extent, for the forward model in the parameter estimation scheme.

Summary

In this work we have, for the first time in the hydrology literature, developed analytical solutions to the problem of groundwater flow in response to evapotranspiration. The solutions developed here are for the saturated zone below the watertable (unconfined aquifers). These solution can be used to invert diurnal groundwater head fluctuations for the daily amplitude of ET flux when the saturated zone is well characterized hydraulically, or conversely, for saturated zone hydraulic parameters when the ET flux at the watertable is well characterized.

In principle, it is also possible to use this solution to estimate both the daily amplitude of ET flux and hydraulic parameters from measurements of diurnal head fluctuations. This has been demonstrated herein by inversion of head fluctuation data from the BHRS and the Larned Research Site for aquifer hydraulic conductivity, the daily amplitude of ET flux and river-stage changes. The models can, in principle, also be used to estimate specific storage and specific yield, as demonstrated by the Larned Research Site example.

For the BHRS example, the hydraulic conductivity estimated with the model developed herein compares well to published values for the research site (Barrash et al., 2006). No direct measurements of ET are available for the research site to which the values determined in this work could be compared. However, values of about 3 mm/day for the ET flux amplitude, seem reasonable for the BHRS. Work is presently underway to measure the ET fluxes at the BHRS using the eddy covariance methods.

For the Larned Research Site, the estimate of ET flux amplitude, $Q = 7.9$ mm/day, obtained in this work compares favorably to the value of $Q = 9.3$ mm/day reported by Butler et al. (2007a) for the 4-day period of July 14–18 in 2003. Butler et al. (2007a) also report that McKay et al. (2004) estimated a specific yield of $S_y = 0.19 - 0.21$, which agrees well with the value obtained herein of $S_y = 0.196$. Butler et al. (2007b) report a conductivity value of $K = 9.1 \times 10^{-4}$ m/s estimated from pumping tests described in Butler et al. (2004). This value is in close agreement with the value estimated with the model developed in this work. There are no published estimates of specific storage at the Larned Research Site to which the value estimated here can be compared. However, it can be stated that the value of $S_s = 5.66 \times 10^{-5} \text{ m}^{-1}$ estimated herein seems reasonable for alluvial deposits of the kind present at the site.

Acknowledgments

The work presented here was supported, in part, by EPA Grant X-960041-01-0. We would like to thank Dr. Warren Barrash for facilitating the use of the Boise Hydrogeophysical Research Site, and Dr. James J. Butler Jr., for providing us with the field data from the Larned Research Site, as well as for providing insightful comments during preparation of the manuscript.

Solution of flow equation

First, one takes the Laplace transform of Eq. (1), leading to

$$p\bar{s}_D = \kappa \frac{\partial^2 \bar{s}_D}{\partial x_D^2} + \frac{\partial^2 \bar{s}_D}{\partial z_D^2}, \quad (\text{A-1})$$

with the boundary conditions given by

$$\lim_{x_D \rightarrow \infty} \bar{s}_D(x_D, z_D, p) = 0, \quad (\text{A-2})$$

$$\left. \frac{\partial \bar{s}_D}{\partial z_D} \right|_{z_D=0} = 0, \quad (\text{A-3})$$

at the base of the aquifer, implying no leakage from the underlying formation, and

$$-\left. \frac{\partial \bar{s}_D}{\partial z_D} \right|_{z_D=1} = \frac{p}{\sigma} \bar{s}_D \Big|_{z_D=1} - \bar{f}_D(p), \quad (\text{A-4})$$

where p is the Laplace transform parameter, $\bar{s}_D = \mathcal{L}\{s_D\}$, $\bar{r}_D = \mathcal{L}\{r_D\}$ and $\bar{f}_D = \mathcal{L}\{f_D\}$.

Semi-infinite flow domain

To solve the flow problem on the semi-infinite domain, simulating an aquifer bounded by a river, one takes the Laplace transform of the river boundary condition, leading to

$$\bar{s}_D(0, z_D, p) = \bar{r}_D(p), \quad (\text{A-5})$$

Next, one takes the Fourier Sine transform of Eqs. (A-1), (A-2), (A-3), (A-4), in x_D , leading to

$$\frac{\partial^2 \bar{s}_D^*}{\partial z_D^2} - \eta^2 \bar{s}_D^* = -\frac{2\xi\kappa}{\pi} \bar{r}_D(p), \quad (\text{A-6})$$

where $\eta^2 = p + \kappa\xi^2$, $\bar{s}_D^* = \mathcal{L}\{\bar{s}\} = \mathcal{L}\mathcal{L}\{s\}$, and the boundary conditions are

$$\left. \frac{\partial \bar{s}_D^*}{\partial z_D} \right|_{z_D=0} = 0, \quad (\text{A-7})$$

and

$$-\left. \frac{\partial \bar{s}_D^*}{\partial z_D} \right|_{z_D=1} = \frac{p}{\sigma} \bar{s}_D^* \Big|_{z_D=1} - \frac{2}{\pi\xi} \bar{f}_D(p). \quad (\text{A-8})$$

The general solution to Eq. (A-6) is

$$\bar{s}_D^* = A + B \cosh(\eta z_D) \quad (\text{A-9})$$

where A and B are constants of integration. Using the boundary conditions in Eqs. (A-7) and (A-8), it follows that

$$A = \frac{2\kappa\xi}{\pi\eta^2} \bar{r}_D(p), \quad (\text{A-10})$$

and

$$B = \left[\frac{2}{\pi\xi} \bar{f}_D(p) - \frac{p}{\sigma} A \right] g(\xi, p). \quad (\text{A-11})$$

Substituting Eqs. (A-10) and (A-11) into Eq. (A-9) leads to Eq. (7)

Infinite flow domain

For the case of an infinite flow domain, one takes the Fourier transform of Eqs. (A-1), (A-2), (A-3), (A-4), leading to

$$\frac{\partial^2 \bar{s}_D^*}{\partial z_D^2} - \eta^2 \bar{s}_D^* = 0, \quad (\text{A-12})$$

and the boundary conditions

$$\frac{\partial \bar{s}_D^*}{\partial z_D} \Big|_{z_D=0} = 0, \quad (\text{A-13})$$

and

$$-\frac{\partial \bar{s}_D^*}{\partial z_D} \Big|_{z_D=1} = \frac{p}{\sigma} \bar{s}_D^* \Big|_{z_D=1} - \frac{\sin(a\xi)}{\pi\xi} \bar{f}_D(p). \quad (\text{A-14})$$

where $\bar{s}_D^* = \mathcal{F}\{\bar{s}\} = \mathcal{L}\mathcal{F}\{s\}$. The general solution to Eq. (A-12) is

$$\bar{s}_D^* = C \cosh(\eta z_D), \quad (\text{A-15})$$

where, according to the boundary conditions,

$$C = \frac{\sin(a\xi)g(\xi, p)}{\pi\xi} \bar{f}_D(p). \quad (\text{A-16})$$

Substituting Eq. (A-16) into Eq. (A-15) leads to Eq. (12).

Depth average of solution

The depth average, $\langle \bar{s}_D^*(\xi, p) \rangle$, of the aquifer response in the transform space is obtained by integrating the point response, $\bar{s}_D^*(\xi, z_D, p)$, across the entire saturated thickness. The integration is defined by

$$\langle \bar{s}_D^*(\xi, p) \rangle = \int_0^1 \bar{s}_D^*(\xi, z_D, p) dz. \quad (\text{B-1})$$

On the semi-infinite flow domain, this integration (averaging), when applied to Eq. (7) leads to

$$\langle \bar{s}_D^*(\xi, p) \rangle = \langle \bar{s}_{D,r}^*(\xi, p) \rangle + \langle \bar{s}_{D,et}^*(\xi, p) \rangle \quad (\text{B-2})$$

where

$$\langle \bar{s}_{D,r}^*(\xi, p) \rangle = \frac{2}{\pi} \frac{\kappa\xi}{\eta^2} \left[1 - \frac{p}{\sigma} \langle \bar{u}_D^*(\xi, p) \rangle \right], \quad (\text{B-3})$$

$$\langle \bar{s}_{D,et}^*(\xi, p) \rangle = \frac{2}{\pi\xi} \langle \bar{u}_D^*(\xi, p) \rangle \bar{f}_D(p), \quad (\text{B-4})$$

and

$$\begin{aligned} \langle \bar{u}_{D,et}^*(\xi, p) \rangle &= \int_0^1 \bar{u}_D^*(\xi, z_D, p) dz = g(\xi, p) \int_0^1 \cosh(\eta z_D) dz \\ &= \frac{g(\xi, p)}{\eta} \sinh(\eta) \end{aligned} \quad (\text{B-5})$$

as in Eq. (18). The same expression for $\langle \bar{u}_{D,et}^*(\xi, p) \rangle$ is obtained when Eq. (12) is integrated with respect to $z \in [0, 1]$. In that case, the depth averaged response, $\langle \bar{s}_{D,et}^*(\xi, p) \rangle$, is given by

$$\langle \bar{s}_{D,et}^*(\xi, p) \rangle = \frac{\sin(a_D \xi)}{\pi\xi} \langle \bar{u}_D^*(\xi, p) \rangle \bar{f}_D(p). \quad (\text{B-6})$$

References

- Abate, J., Valko, P.P., 2004. Multi-precision laplace transform inversion. *International Journal for Numerical Methods in Engineering* 60, 979–993.
- Barrash, W., Clemo, T., 2002. Hierarchical geostatistics and multifacies systems: Boise hydrogeophysical research site, Boise, Idaho. *Water Resources Research* 38 (10), 1196. doi:10.1029/2002WR001436.
- Barrash, W., Reboulet, E., 2004. Significance of porosity for stratigraphy and textural composition in subsurface, coarse fluvial deposits: Boise hydrogeophysical research site. *Geological Society of America Bulletin* 116, 1059–1073. doi:10.1130/B25370.1.
- Barrash, W., Clemo, T., Fox, J.J., Johnson, T.C., 2006. Field, laboratory, and modeling investigation of the skin effect at wells with slotted casing. *Journal of Hydrology* 326 (1–4), 181–198. doi:10.1016/j.jhydrol.2005.10.029.
- Batra, N., Islam, S., Venturini, V., Bisht, G., Jiang, L., 2006. Estimation and comparison of evapotranspiration from MODIS and AVHRR sensors for clear sky days over the southern great plains. *Remote Sensing of Environment* 103, 1–15.
- Bisht, G., Venturini, V., Jiang, L., Islam, S., 2005. Estimation of the net radiation using MODIS (moderate resolution imaging spectro-radiometer) data for clear sky days. *Remote Sensing of Environment* 97, 52–67.
- Butler, J.J., Whittemore, D.O., Zhan, X., Healey, J., 2004. Analysis of two pumping tests at the O'Rourke Bridge site on the Arkansas River in Pawnee County, Kansas. *Kansas Geological Survey Open-File Report 2004-32*, Kansas Geological Survey, Lawrence, Kansas.
- Butler, J.J., Kluitenberg, G.J., Whittemore, D.O., Lodeide II, S.P., Jin, W., Billinger, M.A., Zhan, X., 2007a. A field investigation of phreatophyte-induced fluctuations of the water table. *Water Resources Research* 43, W02404. doi:10.1029/2005WR004627.
- Butler, J.J., Zhan, X., Zlotnik, V.A., 2007b. Pumping-induced drawdown and stream depletion in a leaky aquifer system. *Ground Water* 45 (2), 178–186.
- Cienciala, E., Kučera, J., Malmer, A., 2000. Tree sap flow and stand transpiration of two *Acacia mangium* plantations in Sabah, Borneo. *Journal of Hydrology* 236, 109–120.
- Gribovski, Z., Kalicz, P., Szilágyi, J., Kucsara, M., 2008. Riparian zone evapotranspiration estimation from diurnal groundwater level fluctuations. *Journal of Hydrology* 349, 6–17.
- Lagouarde, J., Brunet, Y., 1993. A simple model for estimating the daily upward longwave surface radiation flux from NOAA-AVHRR data. *International Journal of Remote Sensing* 14 (5), 907–925.
- Loheide, S.P., Butler Jr., J.J., Gorelick, S.M., 2005. Estimation of groundwater consumption by phreatophytes using diurnal watertable fluctuations: a saturated-unsaturated flow assessment. *Water Resources Research* 41, W07030. 10.129/2005WR003942.
- McKay, S.E., Kluitenberg, G.J., Butler Jr., J.J., Zhan, X., Aufman, M.S., Brauchler, R., 2004. In-situ determination of specific yield using soil moisture and water level changes in the riparian zone of the arkansas river, Kansas. *EOS Transaction, AGU* 85 (47), Fall Meeting Supplement, Abstract H31D-0425.
- Moran, M.S., Jackson, R.D., Raymond, L.H., Gay, L.W., Slater, P.N., 1989. Mapping surface energy balance components by combining landsat thematic mapper and ground-based meteorological data. *Remote Sensing of Environment* 30, 77–87.
- Neuman, S.P., 1972. Theory of flow in unconfined aquifers considering delayed response of the water table. *Water Resources Research* 8 (4), 1031–1045.
- Nichols, W.D., 1993. Estimating discharge of shallow groundwater by transpiration from greasewood in the Northern Great Basin. *Water Resources Research* 29 (8), 2771–2778.
- O'Brien, J.J., Oberbauer, S.F., Clark, D.B., 2004. Whole tree xylem sap flow responses to multiple environmental variables in a wet tropical forest. *Plant, Cell and Environment* 27, 551–567.
- Puma, M.J., Celia, M.A., Rodriguez-Iturbe, I., Guswa, A.J., 2005. Functional relationship to describe temporal statistics of soil moisture averaged over different depths. *Advances in Water Resources* 28, 553–566.
- Shah, N., Nachabe, M., Ross, M., 2007. Extinction depth and evapotranspiration from ground water under selected land covers. *Ground Water* 45 (3), 329–338.
- West, E., Ruark, G., 2004. A long, long time ago...: historical evidence of riparian forests in the great plains and how that knowledge can aid with restoration and management. *Journal of Soil and Water Conservation* 59 (5), 105A–110A.
- White, W.N., 1932. A method for estimating ground-water supplies based on discharge by plants and evaporation from soil – results of investigations in the Escalante Valley, Utah. *Tech. Rep. 659-A*, USGS.